

Effect of Cycle Frequency on High-Temperature Oxidation Behavior of Alumina- and Chromia-Forming Alloys

B. A. Pint, P. F. Tortorelli and I. G. Wright

Oak Ridge National Laboratory,
P. O. Box 2008,
Oak Ridge, TN 37831-6156

Abstract

Cycle frequency affects both high-temperature oxidation performance and the method in which the cyclic test is conducted. Several factors are discussed using examples taken from results for Ni-base and Fe-base alumina- and chromia-forming alloys. For the most adherent scales, cycle frequency has little effect on results over extended test times (> 500h). When the scale is less adherent, reducing the cycle time typically has the expected effect of increasing the weight loss per unit exposure time; however, the opposite effect is observed in other cases. Low-cycle frequency experiments can be contained in alumina crucibles. This has the important benefit of collecting the spalled oxide and, for chromia-formers, volatility products. The test method and cycle frequency ultimately have a strong effect on lifetime predictions.

Introduction

Cyclic oxidation testing is one of the fundamental ways to assess high-temperature environmental resistance. Thermal strains that occur during heating and, especially, cooling are often a primary cause of degradation of the external oxide scale that affords protection against further attack¹⁻⁴. The practical reason for this type of test is to simulate application cycles in a controlled manner. Ideally, the cyclic test is designed to mimic the expected duty cycle. However, in a broader sense, it is attractive to use standardized tests that allow direct performance comparisons of different materials and that may provide valuable information for the understanding of cracking and spallation mechanisms⁵⁻¹¹.

Because cyclic oxidation is such a broad topic, this paper attempts to focus on one aspect, cycle frequency or the length of time at temperature for each cycle. Surprisingly, this variable is rarely discussed in any detail¹²⁻¹³. Longer cycle times are of significant importance to projects such as the U.S. Department of Energy's Advanced Turbine Systems Program which is attempting to transfer state-of-the-art materials technology from aircraft engines to land-based gas turbine engines for power generation¹⁴⁻¹⁵. The duty cycle for aircraft is quite different than that for power generation. Consequently, there has been concern that materials and, in particular, coatings which are well-suited for aircraft applications will perform differently in the longer-term cycle experienced in land-based gas turbines, heat exchangers or other power generation technologies.

A second aspect of cycle frequency relates to data collection for lifetime predictions. If more oxidation-resistant alloys (which are generally more expensive) are to be implemented in commercial applications, it is essential to clearly define the expected benefit in life extension that these materials are expected to achieve. Depending on the cycle frequency and the procedures used in conducting the experiment, very different lifetime predictions are possible. Therefore, it is essential to correctly select appropriate test conditions and methods for collecting data in order to develop a reliable prediction.

This paper draws together a wide range of experimental data from a variety of alumina- and chromia-forming alloys in order to illustrate some basic issues regarding cycle frequency and test procedures. In several cases, the testing is still in progress and the results are still evolving. Two forms of testing are

described: uncontained cycling, which is more appropriate for high-frequency tests, and contained cycling, where the specimen is held in an individual alumina crucible which collects spalled and evaporated material (i.e. CrO_3 vapor condenses on the crucible walls). It is demonstrated that, for lifetime predictions, the total weight gain data from contained cycling is more useful than the specimen weight change data alone. However, contained cycling tests are more labor and equipment intensive and are not appropriate for high cycle frequencies and certain exposure conditions.

Experimental Procedure

A variety of alloys were used in this study. Chemical compositions of Ni-base superalloys¹⁶, NiAl variations¹⁷, Pt-containing alloys¹⁸, Fe-base castings¹⁹, ODS FeCrAl^{20,21}, ODS Fe_3Al ²², and ODS NiCr²³ are given in detail elsewhere. Unless otherwise specified, specimens were polished to a $0.3\mu\text{m}$ finish and ultrasonically cleaned in acetone and methanol prior to oxidation.

Short-term (high-frequency) cycles (1-10h) were performed in a computer-controlled cyclic rig in dry flowing O_2 , with seven specimens hanging in a vertical furnace on individual alumina rods and connected to the rod by Pt-Rh wires. Cooling was for 10min to approximately 25°C . Long-term (low-frequency) cycles (100-500h) were conducted in box or horizontal tube furnaces in laboratory air with the specimen contained in a pre-annealed alumina crucible including an alumina lid. Specimens were cooled for at least 24h prior to weighing. Specimens were weighed on a Mettler model AG245 balance. Isothermal kinetics were measured using a Cahn model 1000 microbalance.

This paper focuses on gravimetric results as the principal indicator of the influence of cycle frequency on performance. Little microstructural information is provided, although some conclusions are based on characterizations by metallography, x-ray diffraction, scanning electron microscopy, energy dispersive x-ray spectroscopy (EDS) and transmission electron microscopy.

Results

The experimental results are divided by alloy type in order to demonstrate several important

points about the role of cycle frequency.

Ni-base Superalloys: Sulfur effects

A series of single-crystal Ni-base superalloys based on René N5 were cast in order to investigate the role of Y and S on their oxidation performance¹⁶. Castings without Y were de-sulfurized both in the melt (N5B, N5C and N5D) and by hydrogen annealing (N5AH). While it has been widely observed that de-sulfurization improves performance in high frequency cycles²⁴⁻²⁹, less work has been performed in low frequency cycles¹⁶.

The specimen weight change data from exposures at different cycle times at 1100°C are shown in Figure 1. The 1 and 10h cycles were conducted in an uncontained test while the 100h cycles were conducted in a contained cyclic test. Also, the 10h specimens were only polished to 600grit SiC finish. A number of alloys are shown in order to illustrate that both hydrogen annealing and melt de-sulfurization result in an improvement in scale adhesion relative to a Y-free, nominal sulfur content (4-5ppma) casting (N5A). However, the de-sulfurized alloys differentiated somewhat in the various tests. In particular, N5B (melt de-sulfurized, 2.1ppma S) showed little spallation in 1h cycles but showed progressively higher weight losses with increasing cycle time, Figure 2a. Increasing the cycle time to 100h also resulted in significant spallation for N5C (melt de-sulfurized, 1.8ppma S). The onset of spallation in 100h cycles increased with decreasing sulfur. The standard N5 and N5AH both accumulated more than 3000h of exposure time with only minor spallation.

When the weight losses were large, it was clear from examination of the specimen that spallation was to the metal interface. However, some spallation appeared to only include the outer transient scale, which was typically blue for these alloys. In both 1h and 10h cycles, the specimen weights occasionally made minor but distinct drops in weight (arrows in Figures 1a and 1b) but then continued to gain weight. This was most evident for the castings with more adherent scales, N5 and N5AH, but not for NiAl+Hf (Figure 2a). The result was noticeably lower specimen weights for 1h and 10h cycles compared to 100h cycles (Figure 2b). These drops were attributed to the spallation of the transient Ni-, Co- and Cr-rich scale, e.g. Figure 3, which can spall and still leave behind the underlying, rate-controlling, alumina layer.

These relatively small deviations in specimen mass change make performance comparisons difficult among alloys which do not have large amounts of spallation. One way to try to resolve these differences is to calculate rate constants from the various specimen weights, k_{ps} , Table I. These values can be compared to those from isothermal thermo-gravimetric tests¹⁶, k_{pi} , and to a rate constant calculated from the total weight gain measured for the 100h cycles, k_{pt} . In general, the substrates with more adherent scales (N5, N5AH) also exhibited lower rate constants (a factor of 4-10 compared to N5B and N5C) suggesting that there may be decreased transient scale formation or some type of reactive element (RE) effect³¹⁻³³ occurring in those alloys. While the low-S alloys do not contain Y, they do contain Hf, which has been shown to have a dramatic effect on the scale growth rate in γ -NiAl^{17,18}. It may be an important factor that H₂-annealing removed C as well as S from the superalloy¹⁶, which may affect the Hf activity in the substrate²⁹. Also, the higher rates for N5B and N5C suggest that a thicker alumina scale was forming. This would create higher strains on cooling than alloys with slower scale growth rates.

Overall, there is some benefit associated with comparing these types of calculated rate constants (Table I). However, they provide only qualitative information about relative rates of spallation and are not well suited to incorporation into a quantitative spallation model. One limitation in comparing rates measured under isothermal and cyclic conditions is that the former experiments were run for 100-200h while the latter generally were of 1000h duration. Such a comparison requires a large extrapolation or much longer isothermal tests. The fact that $k_{pi} > k_{pt}$ for the substrates with the most adherent scales suggests that the rate drops with time.

NiAl

When properly doped with a RE such as Zr or Hf, NiAl is one of the most oxidation-resistant alloys. This is clearly illustrated in Figure 2a where NiAl+Hf is observed to show very similar weight gains up to 1000h, independent of cycle frequency. The weight gains were extremely low because of the optimal Hf doping, which has been found to reduce the parabolic rate constant by a factor of 10 or more at this temperature^{17,18}. It is likely that these curves for different cycle frequencies would differentiate but only after much longer times.

The same types of exposures were performed at 1200°C in order to form a thicker oxide, Figure

4. However, there still appeared to be little effect of cycle time up to 1000h, due to the excellent scale adhesion on NiAl+Hf. The observed scatter in the results may be explained by the quality of the NiAl casting. An extreme example is shown with two specimens for 100h cycles, the specimen with the higher weight gain contained cracks in the alloy (which became evident after exposure) while the specimen with the lower weight gain showed no cracks. The higher weight gain including some spallation was attributed to internal oxidation along alloy cracks.

The effect of cycle frequency also was evaluated on undoped NiAl, Figure 5. On the first casting (NiAl-1, Al=50.2at%, 27ppma S), switching from 100h to 1h cycles caused a significant increase in the linear rate of weight loss. After 1000, 1h cycles the specimen had cracked and was forming large amounts of Ni-rich oxide and spinel. A second casting (NiAl-2, Al+51.2at%, 3ppmaS), showed only a slight increase in the linear spallation rates as the cycle frequency was increased from 100h to 1h. The difference in performance between the two castings could be an effect of aluminum content, sulfur content or casting defects. However, it is surprising how little cycle frequency affected the performance of NiAl-2.

Pt-containing alloys

In order to study the role of Pt in aluminides, a series of Pt-containing alloys were cast. Previous papers have reported that these cast (Ni,Pt)Al and PtAl alloys showed little spallation in 1h cyclic testing up to 500h at 1150°C and 100h at 1200°C^{18,28}. This is a considerable improvement over cast, undoped NiAl (e.g., Figure 5) but not as good as that observed for Hf-doped NiAl (Figure 4). However, as illustrated in Figure 6, in 100h cycles at a lower temperature (1100°C) there was no improvement in the total weight gain associated with PtAl or Pt-doped NiAl (2.3at%, 10wt%Pt). After the first 500h, the total weight gains increased nearly linearly, indicating a large amount of spallation similar to that observed for undoped NiAl (50.1at%Al, <4ppmaS). The specimen weight gains (dashed lines) also reflect the spallation from these substrates, with PtAl showing slightly less spallation than NiAl or (Ni,Pt)Al. However, this reduction in specimen weight loss was mainly a result of cracking and internal oxidation of PtAl³⁴ and not due to a more adherent alumina scale.

Total weight gains were also similar for NiAl, PtAl and (Ni,Pt)Al at 1200°C. However, this is not

surprising as the beneficial effect of Pt was only observed for 100, 1h cycles at this temperature, which is only one 100h cycle.

Similar to N5B above, Pt-containing aluminides also showed a reverse effect of cycle frequency, with spallation increasing as frequency decreased. If the role of Pt is to slow the growth of interfacial voids³⁴, this may explain the negative effect of longer cycle time. With a low cycle frequency, the extended time at temperature allows for larger voids to grow at the metal-scale interface³⁵⁻³⁶. Smaller voids formed during shorter cycles may limit the damage to the scale allowing for a healing alumina layer to quickly form, whereas large voids may result in major scale losses. This result is particularly disturbing for Pt-modified aluminide coatings being considered for land-based gas turbine engines. For this long-cycle application, the benefit of Pt additions may be substantially reduced.

Fe-base alloys - difficulty with lifetime predictions

Iron-base alloys show a somewhat different response to cycling than Ni-base alloys. For example, with undoped FeCrAl (20.1at%Cr, 9.6%Al, 85ppma S) in 100h cycles, the performance was nearly identical to NiAl-1/2, Figure 5. This is expected as the scale growth rate is similar on both alloys³³ and essentially all of the oxide spalls after each cycle. When the cycle frequency is increased, the weight loss increases significantly and breakaway oxidation occurs after 550h in 10h cycles, 280h in 2h cycles and 300h in 1h cycles. (All of these specimens were within 5% of a 1.5mm thickness to make this comparison realistic.) The lower Al content relative to NiAl is a major reason for the different behavior of FeCrAl. Particularly in higher frequency cycles, scale spallation from FeCrAl quickly leads to Al depletion and the formation of Fe-rich spinel. This increases the rate of oxide growth and thus higher rates of spallation.

When FeCrAl is doped with Y, there is a well-known strong improvement in scale adhesion^{37,38}. As a result, there is little effect of cycle frequency up to 500h at 1200°C, Figure 7. In 100h cycles, the specimen was run to 5000h with virtually no spalled oxide and only a few cracks observed in the oxide. However, in 1h cycles, the specimen began to crack and deform much earlier and began a continuous weight loss. In both cases the specimen was 1.5mm thick. In 10h cycles, some spallation was observed after 1000h and a specimen in 2h cycles also began to spall after 600h of total exposure.

For iron aluminides, the situation is somewhat different. Two examples are given: a cast alloy, FAL (Fe-28Al-5Cr-0.1Zr) and an oxide-dispersion strengthened substrate, Fe-27Al-2Cr-0.2Y (as Y_2O_3), Figures 8 and 9, respectively. Several papers have pointed out the increased amount of scale spallation for iron aluminides compared to RE-doped FeCrAl or NiAl^{19,22}. In both cases, increasing cycle frequency initially results in more scale spallation. However, unlike Ni-base alloys, the weight loss does not continue linearly. This has been observed both in 1h cycles for FAL and 100h cycles for ODS Fe₃Al.

The observed non-linearity in specimen weight loss is associated with several different phenomena, represented by four different stages in the specimen weight change curve. A general example for Fe-base alloys is given in Figure 10. The first two stages and last stage also are common to Ni-base alloys: the adherent (mass gain) stage followed by linear spallation (mass loss) and finishing with break-away. For Fe-base alloys, however, the rate of linear weight loss often decreases to nearly zero when the alloy begins to form spinel oxide and usually starts to deform. The deformation effect is reflected in the weight loss data for FAL, Figure 8. When a thinner (1mm) specimen was used, the onset of specimen deformation (1000h) was earlier and the weight loss began to level off sooner. A thicker specimen (1.3mm) continued to lose mass after 1700h, although the rate of loss had decreased. Similarly, mass loss was arrested for ODS Fe₃Al during 100h cycles (Fig. 9) when the specimen began to deform and form spinel. An occurrence unique to iron aluminides was the formation of an FeO nodule along the specimen edge which subsequently spalled (arrow in Fig. 8). On FeCrAl specimens, the formation of FeO nodules quickly leads to breakaway oxidation.

Thus, unlike Ni-base alloys such as NiAl and NiCrAl, specimen weight losses in thermal cycling are less well-behaved for Fe-base alloys. This problem is illustrated in Figure 11 for several ODS FeCrAl alloys with a 1.5mm specimen thickness. If the data are examined after only 1000h (dashed line) it is difficult to use this information to accurately rank the long-term performance of the different materials. The commercial Kanthal alloy APM and Y_2O_3 -dispersed FeCrAl appear to be performing similarly, and yet their subsequent behavior is radically different. Likewise, FeCrAl co-doped with Y_2O_3 and Ta_2O_5 appears to be performing very poorly with the largest amount of spallation; yet, it has a longer life than Y_2O_3 -dispersed FeCrAl and performs almost as well as FeCrAl co-doped with TiO_2 . With no general

pattern followed by the various specimens, it is difficult to see how the specimen weight change data could be used in a lifetime prediction model. As a result, the only important number generated by this type of experiment is the time to breakaway (Table II), which, for the best alloys, is much longer than 2000, 1h cycles and therefore involves a large amount of experimental time.

An alternative way to collect similar data is to use a contained cyclic test which yields the total weight gain, Figure 12. The specimen weight change is also obtained (dashed lines) but whereas the specimen weights follow different patterns the total weight gains are reasonably well-behaved. Because the total weight gain is easily correlated with metal wastage, it is much more useful in calculating lifetimes^{19,39-41}.

Chromia-formers

Two examples are given here in order to illustrate some of the issues with chromia-formers and effects at lower temperatures. Figure 13 shows the effect of cycle frequency on an experimental Ni-26at%Cr+0.24Y (as Y₂O₃) alloy at 1000°C. After an initial weight gain for both specimens, the rate of specimen weight loss is greater in 1h cycles. However, no simple conclusion can be reached because of CrO₃ evaporation. The 100h cycles were conducted in alumina crucibles, while the 1h cycles were performed in flowing O₂. Therefore, the greater specimen weight loss may be a result of increased evaporation in the dynamic environment, independent of scale spallation.

Containing a chromia-forming specimen during thermal cycling has a number of benefits. Figure 13 also shows the total weight gain for NiCr+Y during 100h cycles. No spallation was observed in the bottom of the crucible but the inside was green due to the deposited CrO₃ vapor. While in principle some CrO₃ vapor may be lost during the experiment, as the crucible lid is not sealed, no weight losses were recorded during this test. Thus, the difference between the specimen weight change and the total weight gain measured the weight lost due to evaporation.

Total weight gains are, therefore, more reliable for comparing performance at this temperature. The total weight gain for Ni-26Cr+Y is very similar to that for two commercial Y₂O₃-dispersed NiCr alloys (Inco alloy MA754 Ni-21at%Cr and MA758 Ni-33at%Cr) shown as dashed lines in Figure 13. When the dispersion of Y₂O₃ was replaced with La₂O₃ there was a significant drop in the chromia

growth rate²³, Figure 13. Comparing only the specimen weight change data, it is difficult to reach this same conclusion for Ni-26Cr-0.07at%La (as La_2O_3); instead, it could be incorrectly concluded that this alloy spalls more readily than those with Y_2O_3 .

A final example is for foil of Nb-modified Fe-20Cr-25Ni, Figure 14. In this case, contained cycling was used with a cycle time of 500h at various temperatures. The data are shown versus the square root of time in order to emphasize the deviations from parabolic behavior. At the higher temperatures, there was an acceleration in the rate of oxidation but spallation and failure were observed only at 900°C. The acceleration at 800°C was not due to scale spallation (owing to the coincidence of the specimen and total weights) but due to curling and slumping of the foil at a temperature where Nb-modified Fe-20Cr-25Ni has limited strength. One problem with this type of test is noted at 650°C, where the specimen weight gain (dashed line) was higher than the total weight gain (diamond symbols). This was due to the low specimen weight gain and the large difference between the mass of the crucible (12g) and the foil specimen (0.2g). A slight change in the crucible weight due to, for example, outgassing of sintering aid impurities, masks the small specimen weight change in this test. Overall, however, the total weight gain gives a higher confidence to the test data, which are being used to predict foil lifetime⁴².

Discussion

The effect of cycle frequency on oxidation performance is seemingly a very important variable which is rarely discussed in the oxidation literature. It is shown above that the effect of cycle frequency is not consistent for all alloy systems. In some cases, higher cycle frequencies increase oxidation losses, while in others, the opposite effect is observed. A standard explanation would be that there are two broad competing factors when cycle frequency is decreased:

- (1) The frequency of thermal shocking decreases, so that scales that contain defects capable of concentrating the stresses generated in each cooling cycle or acting together to cause fracture are subjected to fewer such events. Also, any defects nucleated by thermal cycling would accumulate at a slower rate.
- (2) The scale and any defects that develop at temperature (such as interfacial voids) have additional time

to grow between thermal shocks. A thicker scale increases the strain that must be accommodated in the cooling cycle and larger defects may increase the amount of spallation.

Thus, increasing the cycle frequency could yield a positive or negative effect on the rate of spallation, and empirically both negative (e.g. NiAl-1, FeCrAl, FeCrAlY, iron aluminides) and positive (e.g. N5B and (Ni,Pt)Al) effects have been observed. However, the more expected result is that increasing the cycle frequency (shorter cycles) should cause far more damage to the scale than low frequency cycles.

Spallation models tend to emphasize the accumulation of damage or defects such as cracks in the scale which lead to spallation. It is commonly assumed that these defects result from thermal cycling. For example, Lowell et al.^{8,9} considered the effects of cycle duration on oxide spallation behavior in the development of an oxidation life-prediction model for superalloys in aircraft engine service. The model assumed that the loss of oxide occurred by spallation within the oxide scale (not to bare metal) in a random fashion over the alloy surface, with the fraction of scale lost in a given segment of the surface being described by one of several statistical distributions. The amount of oxide lost depended on the time available for scale growth between successive spallation events, hence the cycle dwell time was an important parameter. The model predicted that decreasing the cycle frequency would increase maximum weight change and decrease the number of cycles to net scale spallation. Their data for Ni-30Cr showed this effect when weight change in cycles from 5-300min versus *number of cycles* was plotted. However, when the data are replotted versus *time at temperature*, cycles from 5-60min showed no difference, and only for 5h cycles was there less spallation. This is similar to the small effect observed in this study between 1h and 2h cycles, Figures 5, 8 and 9.

The negative effect of decreasing cycle frequency (i.e. more spallation with longer time cycles) perhaps requires a different type of mechanism than what is described by Lowell et al.. There are processes which occur isothermally, such as oxidation-induced deformation of the substrate and growth of interfacial voids and dopant-rich oxides (such as Ta-rich oxides on superalloys¹⁶) which may have different effects when the cycle frequency is changed. Allowing these defects to increase in size (by increasing the length of the cycle) may change the spallation event from a localized minor event, such as that nucleated by a small defect, to a much larger event affecting a large fraction of the scale. The specific

mechanisms by which each type of material reacts to a change in the cycle frequency is beyond the scope of this paper. Future work in this area should include extensive characterization work, including a time-series of specimens.

The time at which the effect of cycle frequency begins to differentiate appears to be a strong function of substrate scale adhesion. For NiAl+Hf, that time exceeds 1000h at 1200°C, compared to about 500h for FeCrAlY, 100h for iron aluminides and very short times for most undoped alumina-formers. This result is not surprising, because until the scale starts to spall it grows at a rate essentially equal to that under isothermal conditions. This critical time is an important factor in terms of experimental design. Only by exceeding the critical time can the effect of cycle frequency be evaluated. For example, the effect of cycle frequency is not known for NiAl+Hf because the experiments have not been run for a sufficiently long time.

Another point to emphasize is the shape of the specimen weight gain curve. In general, the Ni-base alloys exhibit more regular behavior, with a protective period followed by a nearly-linear weight loss period when the alloy begins to spall, Figures 1, 2, 5 and 6. This type of behavior has been successfully modeled by workers at the NASA Lewis Research Center^{8,9,43-45} and others⁴⁶. However, this type of behavior is not as clearly observed in Fe-base alloys which were not included in these previous modeling efforts. As illustrated in Figure 10, the spallation curves often have a nearly zero rate loss period not observed in Ni-base alloys. Even this figure is an oversimplification, as there is a wide variety of behaviors, as shown in Figure 11. This complication makes it difficult to apply models such as those developed for Ni-base alloys to Fe-base alloys. As suggested by the data in Figure 12, it may be easier to model lifetime if the total weight gain is collected in a contained cyclic test, rather than only the specimen weight change in an uncontained test. The total weight gain curves are easily fitted to an exponential or other function to predict lifetimes.

Thus, an important underlying issue on the effect of cycle frequency concerns the method by which the test is conducted. There are two general methods; both have strengths and weaknesses, depending on the goals of the test:

Uncontained Testing

This type of experiment is characterized by specimens hanging in a furnace or otherwise not self-contained in a crucible and is more widely observed in the oxidation literature. One of the benefits of this type of test is that it is more flexible and easier to conduct. This method is also preferred for complex environments, such as mixed gas or water vapor, where it is necessary to ensure that the specimen experiences a constant gas composition and gas velocity may be a variable. With a computer-controlled cyclic rig, essentially any cycle time can be used and cooling can be easily modified by the rate of withdrawal or by using fan cooling upon removal from the furnace. In any case, heating and cooling times are relatively short. However, one of the important failings of this type of test is that it is very difficult to know the total weight gain; when the specimen spalls its scale, only the specimen weight change can be accurately measured. This appears to be less of a problem for Ni-base alloys which appear to be more well-behaved than Fe-base alloys.

Sources of error for this test are the evaporation of the Pt-Rh attachment wire (for a 2cm long, 0.5mm diameter wire this can vary from $0.4\mu\text{gh}^{-1}$ at 1000°C to $12\mu\text{gh}^{-1}$ at 1200°C in flowing O_2) and the uncertainty regarding chromia volatilization versus spallation for weight losses of chromia formers (e.g. Figure 13). Also, depending on the friability of the scale, there may be more or less scale lost from the specimen depending on how it is handled, particularly while being weighed.

Contained Testing

This type of test is characterized by individual crucibles with lids to contain any spalled or volatile CrO_3 products. Without the lid, the validity of the test is far more questionable. The primary benefit of this test is that it yields the total weight gain (including spallation products) and appears to retain most evaporated chromia on the crucible walls and lid. This allows better assessments of relative metal consumption rates than are possible from the specimen weight change alone. The amount of spallation or evaporation is directly quantified without any required assumptions and is collected in the crucible if analysis is required.

There are several limitations of contained testing. First, because of the large thermal mass and problem of thermal shock of alumina, short cycles are impractical. Also, when a set of multiple crucibles are inserted into a tube furnace, the furnace temperature is often altered for 30min or more. For 1h or 2h

cycles this would cause a significant difference in the thermal history of the specimen compared to uncontained tests or longer cycles. This test is best suited for 10h or longer to avoid such problems.

Because the specimen is isolated in a crucible, it is difficult to use environments other than air with this test. With increased emphasis on the effect of mixed gas environments and particularly water vapor in combustion environments, this is a significant limitation. For iron aluminides, which can exhibit accelerated oxidation in air compared to O₂^{19,47} this is also a concern. Another drawback of this test is that weighing the crucible, the specimen and then the crucible without the specimen (as a check) is much more time consuming than merely weighing the specimen. The alumina crucibles are also an added expense, although they rarely need to be replaced. The specimen size is also restricted by the size of the crucible.

The sources of error in this test are more varied. One factor is that an alumina crucible mass (10-13g) is often an order of magnitude larger than the specimen (1-2g). As pointed out for low specimen weight gains (650°C in Figure 14), slight changes in the crucible weight can distort the total weight gain. This problem can be corrected in a similar manner to the evaporation of Pt, and is most strongly encountered after the first cycle. For well-used crucibles, weight changes (mainly slight losses) are typically 0.1mg per 1000h of usage. In general, for weight changes like those observed at 1200°C (Figure 12) this error is extremely small.

Additional precautions are the use of gloves when handling crucibles to prevent transfer of contaminants onto the crucible surface. Also, if the crucible contents are spilled, re-weighing and corrections may be required. The total weight gain only decreases in value in extremely rare circumstances. Independent of specimen and cycle conditions, the total weight gain should increase after every cycle. Finally, the assumption that no CrO₃ vapor is lost from a crucible with a lid has not been tested. Comparisons with sealed crucibles would help in addressing this issue.

Conclusions

As is readily apparent in this paper, the issue of cycle frequency is far from resolved but a number of important points can be emphasized. First, the effect of cycle frequency is not uniform. It is high-

ly dependent on the scale adherence to the substrate, the total test time and (likely) the test temperature. Cycle frequency also affects how the test is performed, as longer term cycles (100h) are better suited for contained testing in alumina crucibles and shorter cycles (1-2h) require uncontained testing. In general, the objectives of the testing strongly influence the test procedures. For life prediction, total weight gain from contained testing appears to be very valuable and reliable, particularly for Fe-base alloys which perform somewhat differently than Ni-base alloys. Further work will be required to fully understand the issue of cycle frequency and its implications on high-temperature oxidation performance.

Acknowledgments

The authors are indebted to M. J. Bennett (formerly of Harwell Laboratory, UK) who started us on our program on contained cyclic testing. The authors also would like to thank M. Howell, L. D. Chitwood, G. Garner, N. Bonwit and C. Roberts at ORNL for many hours of assistance with the experimental work and J. R. DiStefano, **D. F. Wilson**, and **J. A. Haynes** at ORNL for their comments on the manuscript. This research was sponsored by the U.S. Department of Energy, **Fossil Energy AR&TD Materials Program and the Advanced Turbine Systems program** under contract DE-AC05-96OR22464 with Lockheed Martin Energy Research Corporation.

References

1. C. A. Barrett and E. B. Evans, *Am. Ceram. Soc. Bull.*, 1973, 52, 353-60.
2. C. E. Lowell and D. L. Deadmore, *Oxid. Met.*, 1980, 14, 325-36.
3. R. Mevrel, *Mat. Sci. Tech.*, 1987, 3, 531-5.
4. M. Schütze, *Protective Oxides Scales and Their Breakdown*, J. Wiley and Sons, Chicester, UK, 1997.
5. H. Jonas and J. A. Golczewski, *J. Nucl. Mater.*, 1984, 120, 272-7.
6. H. E. Evans, *Mater. Sci. Tech.*, 1988, 4, 415-20.
7. P. Hancock and J. R. Nicholls, *Mat. Sci. Tech.*, 1988, 4, 398-406.
8. M. J. Bennett, H. E. Evans and D. A. Shores, *Mat. High Temp.*, 1994, 12, 127-33.
9. J. Jedlinski, M. J. Bennett and H. E. Evans, *Mat. High Temp.*, 1994, 12, 169-75.
10. H. E. Evans, J. R. Nicholls and S. R. J. Saunders, *Solid State Phenom.*, 1995, 41, 137-56.
11. J. R. Nicholls, H. E. Evans and S. R. J. Saunders, *Mat. High Temp.*, 1997, 14, 5-13.
12. C. E. Lowell, S. R. Levine, and S. J. Grisaffe, in *Proc. 1974 Gas Turbine Materials in the Marine Environment Conference*, MCIC Report No. 75-27, pp.535-554, Metals and Ceramics

- Information Center, Battelle, Columbus, Ohio, 1975.
13. C. E. Lowell, J. M. Smialek, and C. A. Barrett, in *High-Temperature Corrosion*, pp. 219-226, R. A. Rapp, Ed., NACE, Houston, TX, 1983.
 14. "Comprehensive Program Plan for Advanced Turbine Systems," Office of Fossil Energy and Office of Energy Efficiency and Renewable Energy, Department of Energy, Report to Congress No. DOE/FE-0279, July 1993.
 15. W. P. Parks, E. E. Hoffman, W. Y. Lee, and I. G. Wright, *J. Thermal Spray*, 1997, 6, 187-192.
 16. I. G. Wright, B. A. Pint, W. Y. Lee, K. B. Alexander and K. Prüßner, in *High Temperature Surface Engineering*, **in press**, J. Nicholls, ed., Institute of Materials, London, UK, 1999.
 17. B. A. Pint, *Oxid. Met.*, 1998, 49, 531-60.
 18. B. A. Pint, I. G. Wright, W. Y. Lee, Y. Zhang, K. Prüßner and K. B. Alexander, *Mater. Sci. Eng.*, 1998, A245, 201-11.
 19. B. A. Pint, P. F. Tortorelli and I. G. Wright, *Mater. High Temp.*, 1999, in press.
 20. B. A. Pint and K. B. Alexander, *J. Electrochem. Soc.*, 1998, 145, 1819-29.
 21. B. A. Pint, "A Quantification of Dopant Effects in ODS FeCrAl," for submission to *Oxid. Met.*.
 22. B. A. Pint, P. F. Tortorelli and I. G. Wright, *Mater. Corr.*, 1996, 47, 663-74.
 23. B. A. Pint, C. R. Roberts and I. G. Wright, "The Effect of Dopant Ion Size on the Oxidation Behavior of Oxide-Dispersed NiCr Alloys", manuscript in progress.
 24. A. W. Funkenbush, J. G. Smeggil and N. S. Bornstein, *Met. Trans.*, 1985, 16A, 1164-6.
 25. J. L. Smialek, D. T. Jayne, J. C. Schaeffer and W. H. Murphy, *Thin Solid Films*, 1994, 253, 285-92.
 26. J. L. Smialek and B. K. Tubbs, *Met. Trans.*, 1995, 26A, 427-35.
 27. G. H. Meier, F. S. Pettit and J. L. Smialek, *Werk. Korr.*, 1995, 46, 232-40.
 28. M. A. Smith, W. E. Frazier and B. A. Pregger, *Mat. Sci. Eng.*, 1995, A203, 388-398.
 29. C. Sarioglu, C. Stinner, J. R. Blachere, N. Birks, F. S. Pettit and G. H. Meier, in *Superalloys 1996*, pp.71-80, R. D. Kissinger, D. J. Deye, D. L. Anton, A. D. Cetel, M. V. Nathal, T. M. Pollack and D. A. Woodford Eds., TMS, Warrendale, PA, 1996.
 30. K. Prüßner and I. G. Wright, unpublished research 1998.
 31. D. P. Moon, *Mater. Sci. Tech.*, 1989, 5, 754-64.
 32. A. Strawbridge and P. Y. Hou, *Mater. High Temp.*, 1994, 12, 177-81.
 33. B. A. Pint, *Oxid. Met.*, 1996, 45, 1-37.
 34. E. C. Dickey, B. A. Pint, K. B. Alexander and I. G. Wright, submitted to *J. Mater. Res.*, 1999.
 35. J. L. Smialek, *Met. Trans.*, 1978, 9A, 309-20.
 36. B. A. Pint, *Oxid. Met.*, 1997, 48, 303-28.
 37. C. S. Wukusick and J. F. Collins, *Mater. Res. Stand.*, 1964, 4, 637-46.
 38. F. A. Golightly, F. H. Stott and G. C. Wood, *J. Electrochem. Soc.*, 1979, 126, 1035-42.
 39. W. J. Quadackers and M. J. Bennett, *Mat. Sci. Tech.*, 1994, 10, 126-31.
 40. W. J. Quadackers and K. Bongartz, *Werkst. Korros.*, 1994, 45, 232-41.
 41. I. G. Wright, B. A. Pint, C. S. Simpson and P. F. Tortorelli, *Mater. Sci. Forum*, 1997, 251-4, 195-202.
 42. B. A. Pint, P. F. Tortorelli and I. G. Wright, unpublished research, 1998.
 43. J. A. Nesbitt, *J. Electrochem. Soc.*, 1989, 136, 1511-7 & 1518-27.
 44. **C. E. Lowell, C. A. Barrett, R. W. Palmer, J. V. Auping and H. B. Probst, *Oxid. Met.*, 1991, 36, 81-112.**
 45. J. A. Nesbitt, E. J. Vinarcik, C. A. Barrett, and J. Doychak, *Mater. Sci. Eng.*, 1992, A153, 561-6.

46. K. S. Chan, N. S. Cheruvu and G. R. Levant, ASME 97-GT-389.
47. B. A. Pint, J. Regina, K. Prüßner, L. D. Chitwood, K. B. Alexander, and P. F. Tortorelli, submitted to *Intermetallics*, 1999.

List of Figures

Figure 1. Weight gain for several single crystal Ni-base superalloys oxidized at 1100°C in (a) 1h, (b) 10h and (c) 100h cycles. Removing indigenous sulfur in the melt or by hydrogen annealing improved scale adhesion, but not always to the same degree. Alloy N5B with 2.1ppmaS did not lose weight in 1h cycles but did in 10h and 100h cycles. In shorter cycles (a) and (b), arrows mark specimen losses not followed by continued weight loss. These events are linked to the spallation of the transient Ni-rich outer scale and not to spallation of the alumina scale.

Figure 2. Weight gain for various cycle times at 1100°C for (a) N5B and NiAl+Hf and (b) standard N5 (with Y) and hydrogen annealed N5, N5AH. With increasing cycle frequency the scale spallation decreased for N5B but showed little effect on NiAl+Hf. The lower weight gains in shorter time cycles for N5 and N5AH likely reflects spallation of the transient oxide. In 100h cycles, N5 and N5AH still show little spallation.

Figure 3. SEM back-scattered electron image of the scale formed on N5AH after 100h at 1200°C in a polished cross-sectional mount. The transient scale formed at the gas-side interface contains predominantly Ni, Co and Cr and has begun to spall without obvious defects in the underlying alumina scale. The very bright particles are rich in Ta as determined by EDS analysis³⁰.

Figure 4. Specimen weight gain for NiAl+0.05at%Hf for various cycle times at 1200°C. For the slow-growing and very adherent alumina scale formed on Hf-doped NiAl, much longer times will be required to determine the effect of cycle frequency. Some variability was observed which may be related to the quality of the NiAl casting. In 100h cycles, a higher weight gain was noted when the specimen contained several cracks.

Figure 5. Specimen weight gain for undoped FeCrAl and undoped NiAl as a function of cycle time at 1200°C. In 100h cycles, all alloys behaved similarly with an alumina scale forming and spalling after each cycle. In 1h cycles, spallation was more severe for FeCrAl but there was wide variability for two different near-stoichiometry NiAl alloys. Curves for FeCrAl end at breakaway for 1,2 and 10h cycles. For NiAl-2, cycle frequency had little effect on spallation rate.

Figure 6. Specimen (dashed line) and total weight gains (symbols) for several aluminides during 100h cycles in crucibles at 1100°C in air. A beneficial effect of Pt was not observed when the cycle time was increased to 100h; however, Hf-doped NiAl showed no spallation.

Figure 7. Specimen weight gain for 1.5mm thick FeCrAlY as a function of cycle time at 1200°C. For the very adherent alumina scale formed on FeCrAlY, 600h was required to begin differentiation between 1h and 100h cycles. After 5000h in 100h cycles, virtually no scale spallation was observed.

Figure 8. Specimen weight gain for cast/extruded FAL as a function of cycle time at 1200°C. After 200h, higher cycle frequency resulted in a significant increase in the amount of specimen weight loss. This behavior also was affected by specimen thickness. At one point (arrow), the specimen appeared to begin breakaway oxidation but the affected area broke off and the specimen continued for several hundred hours. This type of behavior was not observed for FeCrAl alloys.

Figure 9. Specimen weight gain for 1.5mm thick ODS Fe₃Al as a function of cycle time at 1200°C. Initially, a lower cycle frequency resulted in less specimen weight loss with time. In 1h cycles, weight loss was arrested when the specimen began to deform and form spinel.

Figure 10. Representative example of specimen weight change for Fe-base alumina-forming alloys in 1h cycles at 1200°C. Behavior tends to follow four periods: (1) adherent oxide formation, i.e. no spallation with weight gains comparable to those measured isothermally; (2) onset of spallation, sometimes following a linear loss, like that observed for Ni-base alloys; (3) substrate deformation (warping or curving) usually accompanied by spinel formation and specimen no longer losing weight and, finally, gaining weight prior to (4) breakaway oxidation, i.e the formation of FeO.

Figure 11. Specimen weight gain for 1.5mm thick FeCrAl alloys in 1h cycles at 1200°C. No simple relationship can explain the range of behaviors observed. Lifetime predictions based on 1000h (dashed line) would fail to predict the behavior of most of these materials. For example, FeCrAl co-doped with 0.1at% Y₂O₃ and 0.1at% Ta₂O₅ initially lost a significant amount of weight but lasted as long as the alloy co-doped with TiO₂. The best alloys require even longer times to begin spallation.

Figure 12. Total and specimen weight gains for several Fe-base alloys in 100h cycles at 1200°C. Whereas there were various behaviors for the specimen weight change, the total weight gains were more well-behaved. The total weight gain is directly proportional to the metal wastage and, therefore, can be used to predict lifetime. No spallation was observed for FeCrAlY as the total and specimen weight gains coincided.

Figure 13. Total and specimen weight gains for several ODS NiCr alloys at 1000°C. In 100h crucible test, specimen weight loss (relative to the total weight gain) for Ni-26at%Cr+Y₂O₃ and Ni-26Cr+La₂O₃ was attributed solely to CrO₃ evaporation, as no spallation was observed in the crucible. In 1h uncontained cycles, more weight loss was observed, whether this was due to enhanced evaporation outside a crucible or increased spallation is not known. Total weight gains for commercial Y₂O₃-dispersed NiCr alloys MA754 and MA758 are shown to confirm the normal behavior of Y-doped NiCr and the superior performance with La-doping.

Figure 14. Weight gain for Fe-20Cr-25Ni+Nb 100μm foil at several temperatures plotted against the square root of time to show the parabolic relationship. The diamonds mark the total weight gain in 500h cycles and the dashed line is the specimen weight gain. Except at 900°C, there was little spallation observed. At 650°C, the total was less than the specimen weight because of an experimental problem.

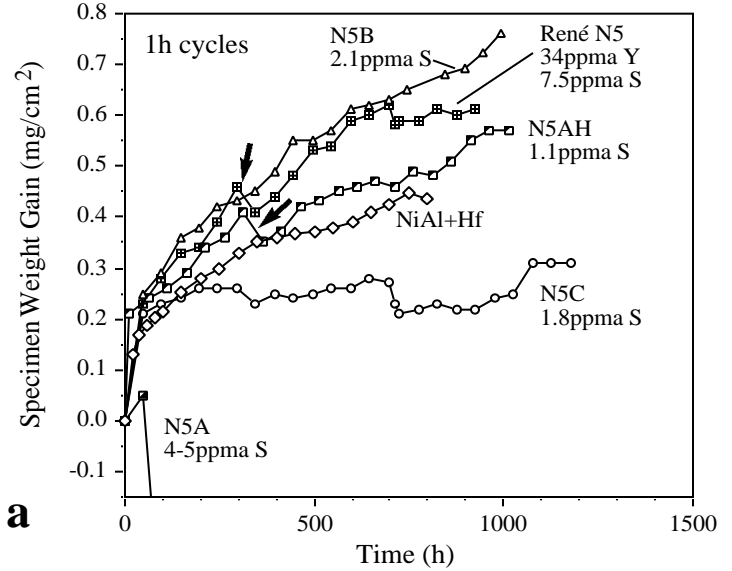
Table I. Parabolic rate constants, $\text{g}^2\text{cm}^{-4}\text{s}^{-1}$ ($\times 10^{-14}$) at 1100°C for variations of René N5, a single crystal Ni-base superalloy, for different cycle times and isothermally.

Alloy Comments	Calculated From						
	Specimen		W				
(k_{ps})			Total	W			
(k_{pt})			Iso-thermal				
(k_{pi})			1h	10h	100h*	100h	100h
-NiAl-Hf N5	cast,0.05at% Hf		4.5	3.3	2.9 (6)	2.7	11.4
					standard		
34ppma Y, 7.5ppma S			10.4	7.1	6.8 (42)	14.1	31.6
N5A					No Y,		
4-5ppma S	—		—	—	11,800	132	
N5B	No Y, 2.1ppma S		13.1	—	(40)	64.5	44.7
N5C	No Y, 1.8ppma S		—	13.6	(72)	58.5	62.1
N5AH					H ₂ -annealed		
No Y,1.1ppma S			5.9	3.2	4.9 (32)	5.9	35.7

*values in parenthesis estimated from first 200-300h data

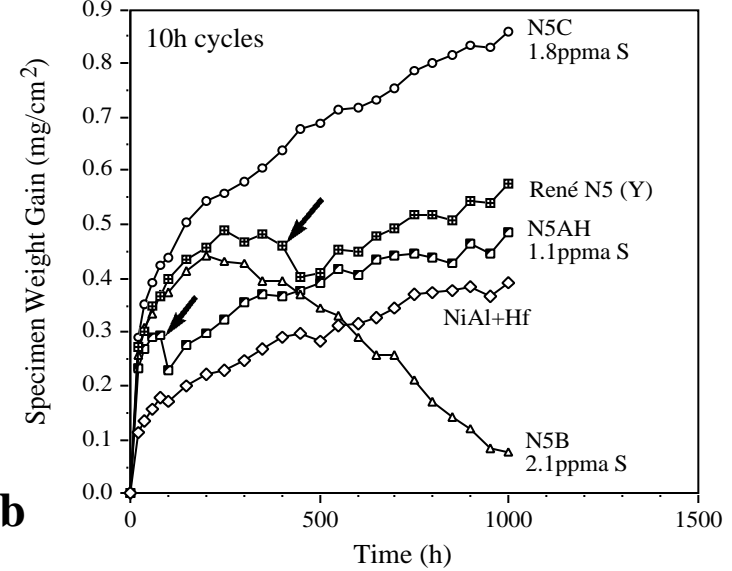
Table II. Normalized life in 1h cycles at 1200°C for various Fe-base alloys extrapolated to a uniform 1.5mm specimen thickness. Many of the tests are still being run to completion.

Alloy Thickness (mm)	Actual Normalized Life	
	1h cycles, 1200°C	
1.5mm thickness		
Fe-28Al-2Cr	1.0	2500
FAL	1.0	3450
FAL	1.3	>2100
FAP	0.9	1270
PMWY2A	1.5	>1900
FeCrAl	1.5	310
FeCrAlY	1.5	>1950
PM2000	1.7	>1700
APM	1.2	>3050
FeCrAl+Y ₂ O ₃	1.4	1570
FeCrAl+La ₂ O ₃	1.4	2400
FeCrAl+HfO ₂	1.5	>2400
FeCrAl+SrO	1.5	>2700

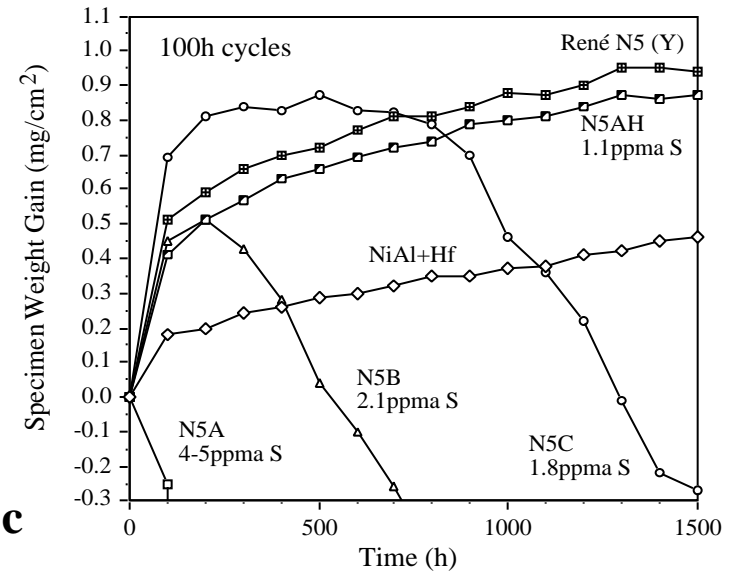


a

Figure 1. Weight gain for several single crystal Ni-base superalloys oxidized at 1100°C in (a) 1h, (b) 10h and (c) 100h cycles. Removing indigenous sulfur in the melt or by hydrogen annealing improved scale adhesion, but not always to the same degree. Alloy N5B with 2.1ppmaS did not lose weight in 1h cycles but did in 10h and 100h cycles. In shorter cycles (a) and (b), arrows mark specimen losses not followed by continued weight loss. These events are linked to the spallation of the transient Ni-rich outer scale and not to spallation of the alumina scale.



b



c

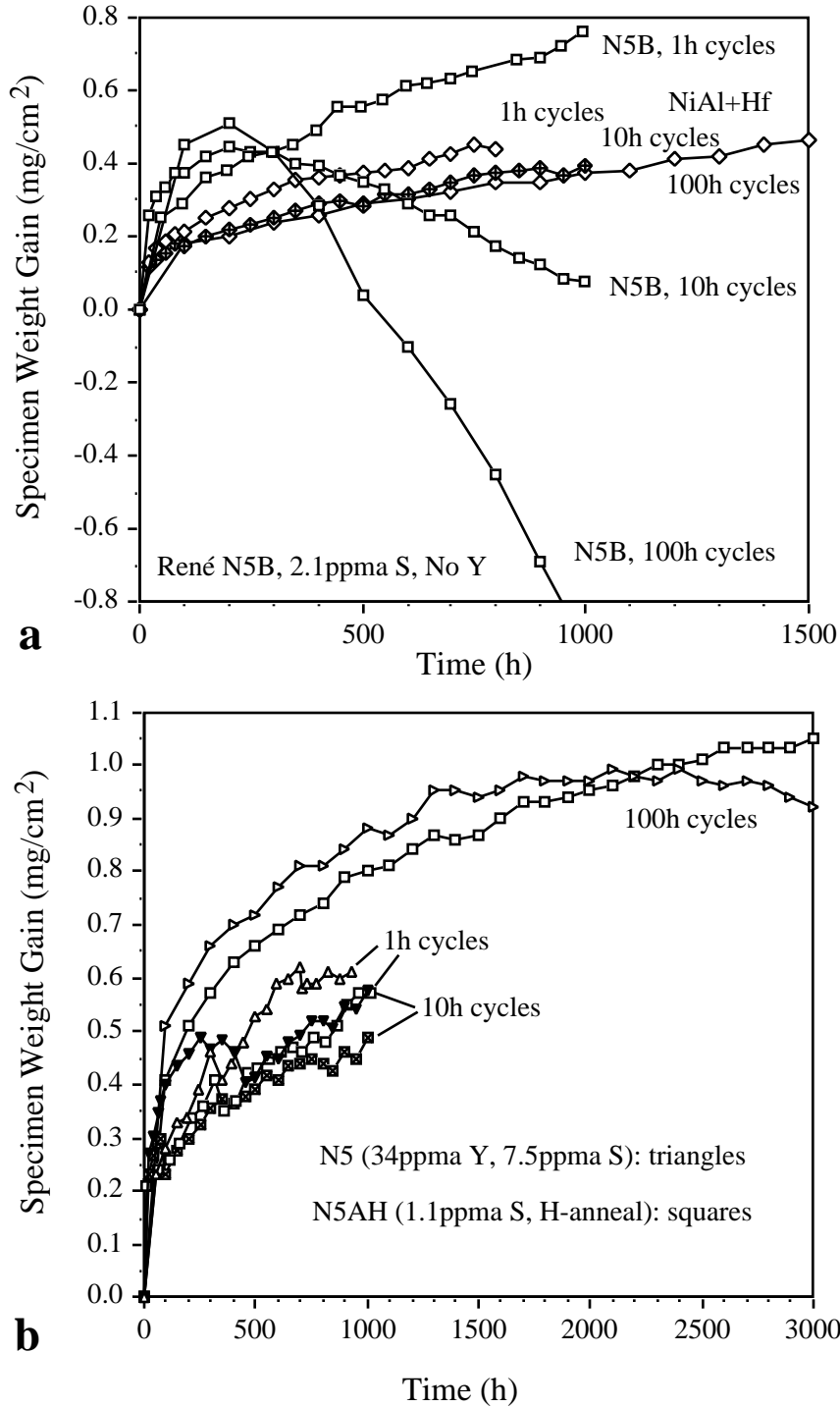


Figure 2. Weight gain for various cycle times at 1100°C for (a) N5B and NiAl+Hf and (b) standard N5 (with Y) and hydrogen annealed N5, N5AH. With increasing cycle frequency the scale spallation decreased for N5B but showed little effect on NiAl+Hf. The lower weight gains in shorter time cycles for N5 and N5AH likely reflects spallation of the transient oxide. In 100h cycles, N5 and N5AH still show little spallation.

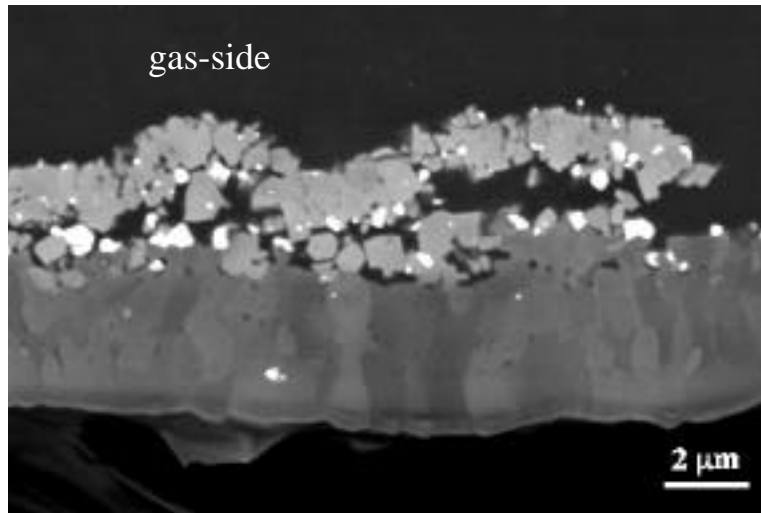


Figure 3. SEM back-scattered electron image of the scale formed on N5AH after 100h at 1200°C in a polished cross-sectional mount. The transient scale formed at the gas-side interface contains predominantly Ni, Co and Cr and has begun to spall without obvious defects in the underlying alumina scale. The very bright particles are rich in Ta as determined by EDS analysis³⁰.

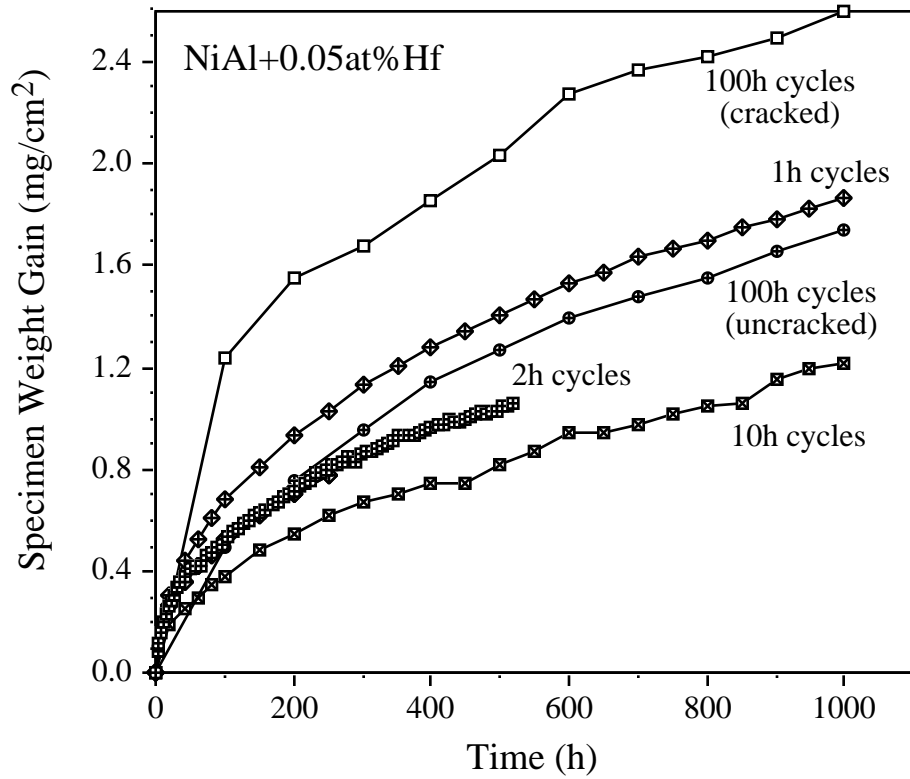


Figure 4. Specimen weight gain for NiAl+0.05at%Hf for various cycle times at 1200°C. For the slow-growing and very adherent alumina scale formed on Hf-doped NiAl, much longer times will be required to determine the effect of cycle frequency. Some variability was observed which may be related to the quality of the NiAl casting. In 100h cycles, a higher weight gain was noted when the specimen contained several cracks.

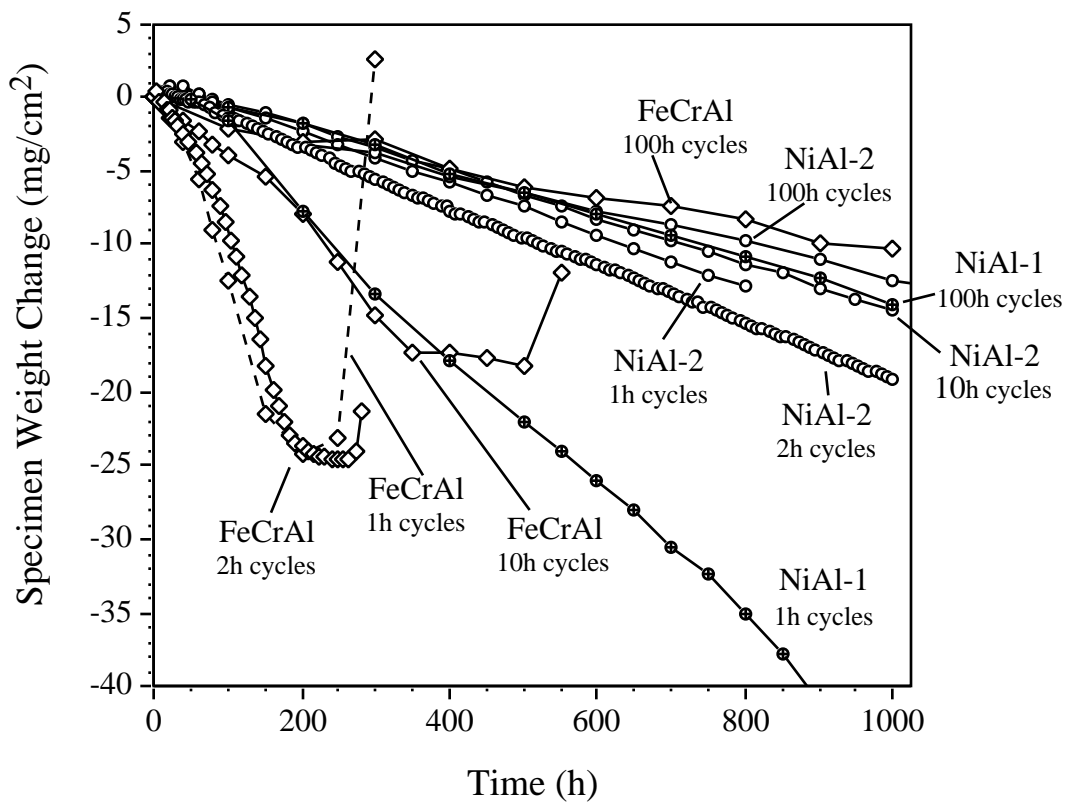


Figure 5. Specimen weight gain for undoped FeCrAl and undoped NiAl as a function of cycle time at 1200°C. In 100h cycles, all alloys behaved similarly with an alumina scale forming and spalling after each cycle. In 1h cycles, spallation was more severe for FeCrAl but there was wide variability for two different near-stoichiometry NiAl alloys. Curves for FeCrAl end at breakaway for 1,2 and 10h cycles. For NiAl-2, cycle frequency had little effect on spallation rate.

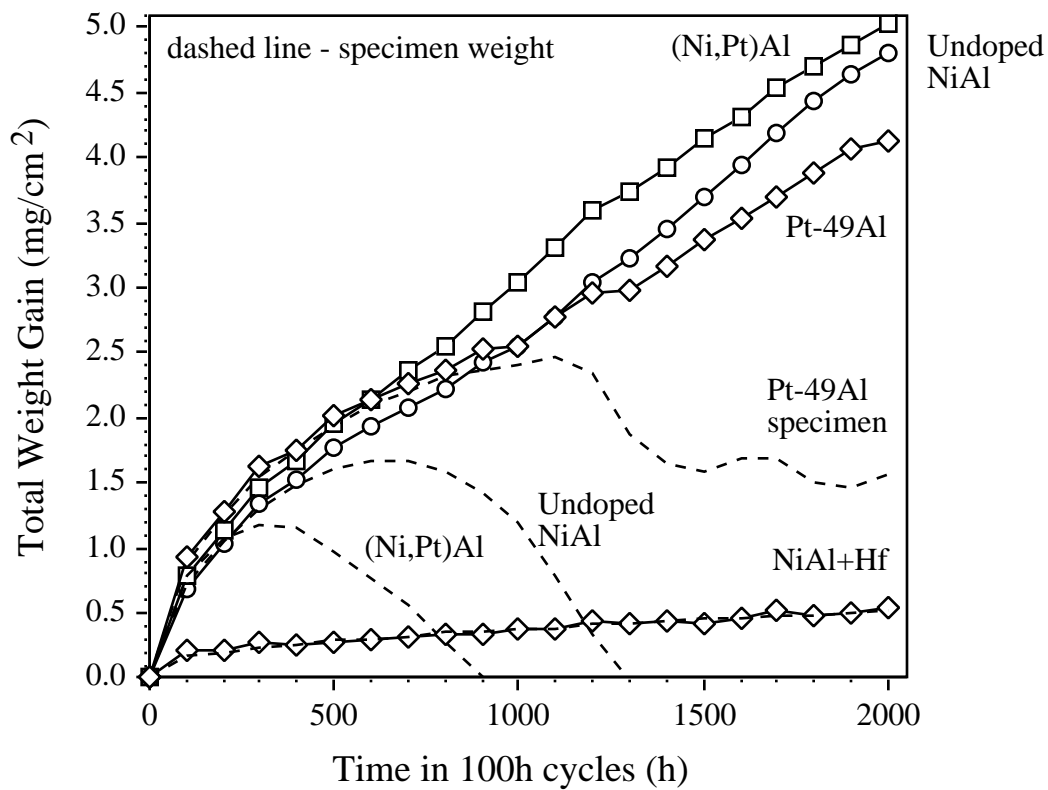


Figure 6. Specimen (dashed line) and total weight gains (symbols) for several aluminides during 100h cycles in crucibles at 1100°C in air. A beneficial effect of Pt was not observed when the cycle time was increased to 100h; however, Hf-doped NiAl showed no spallation.

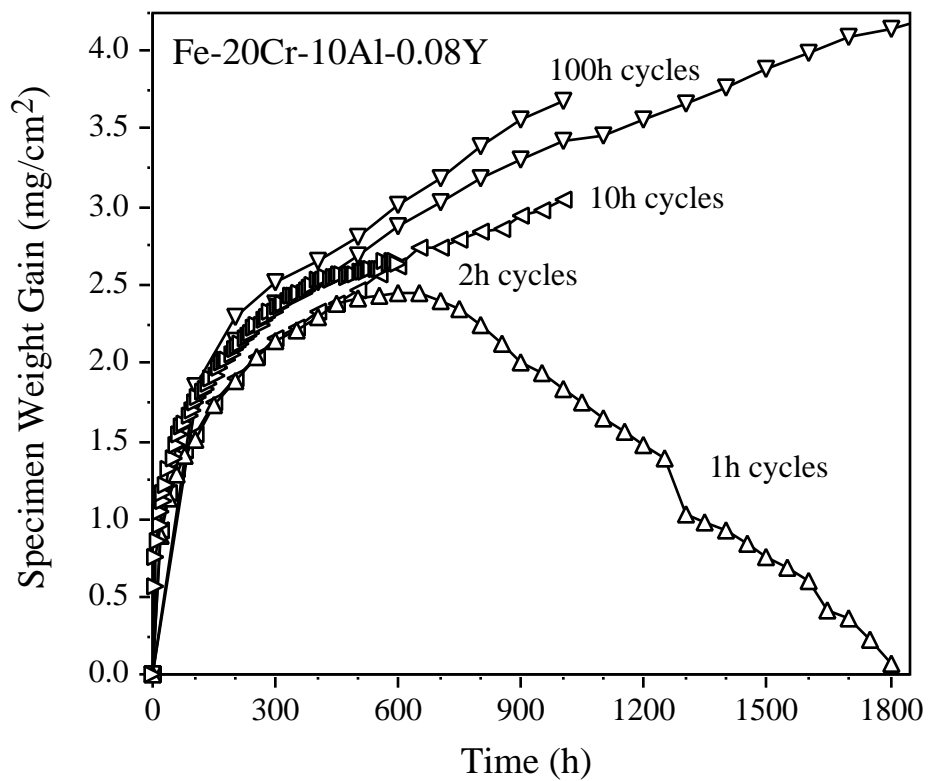


Figure 7. Specimen weight gain for 1.5mm thick FeCrAlY as a function of cycle time at 1200°C. For the very adherent alumina scale formed on FeCrAlY, 600h was required to begin differentiation between 1h and 100h cycles. After 5000h in 100h cycles, virtually no scale spallation was observed.

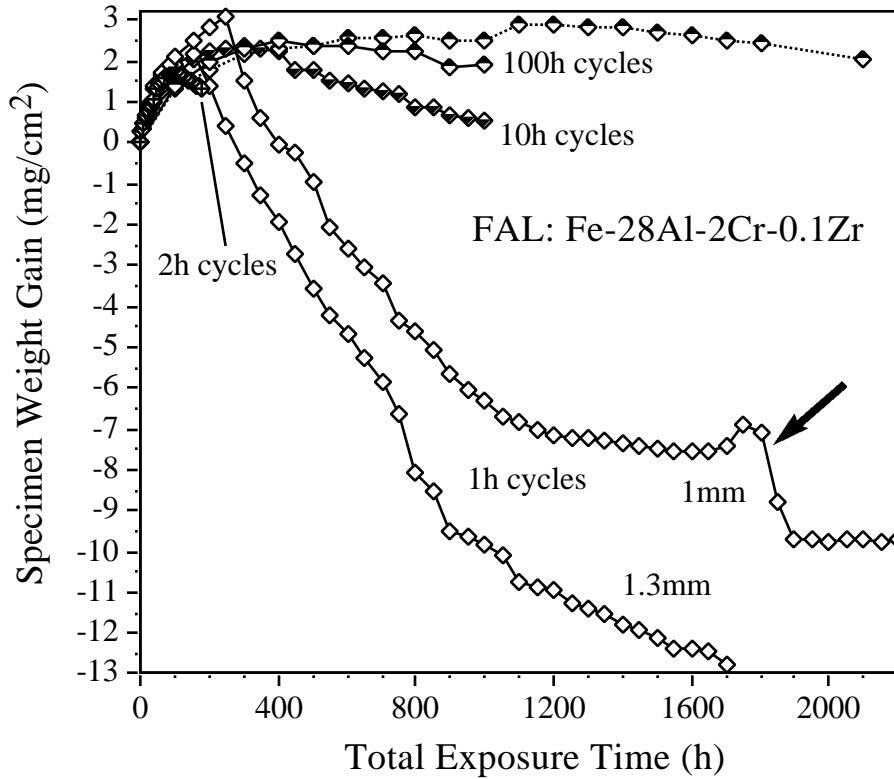


Figure 8. Specimen weight gain for cast/extruded FAL as a function of cycle time at 1200°C. After 200h, higher cycle frequency resulted in a significant increase in the amount of specimen weight loss. This behavior also was affected by specimen thickness. At one point (arrow), the specimen appeared to begin breakaway oxidation but the affected area broke off and the specimen continued for several hundred hours. This type of behavior was not observed for FeCrAl alloys.

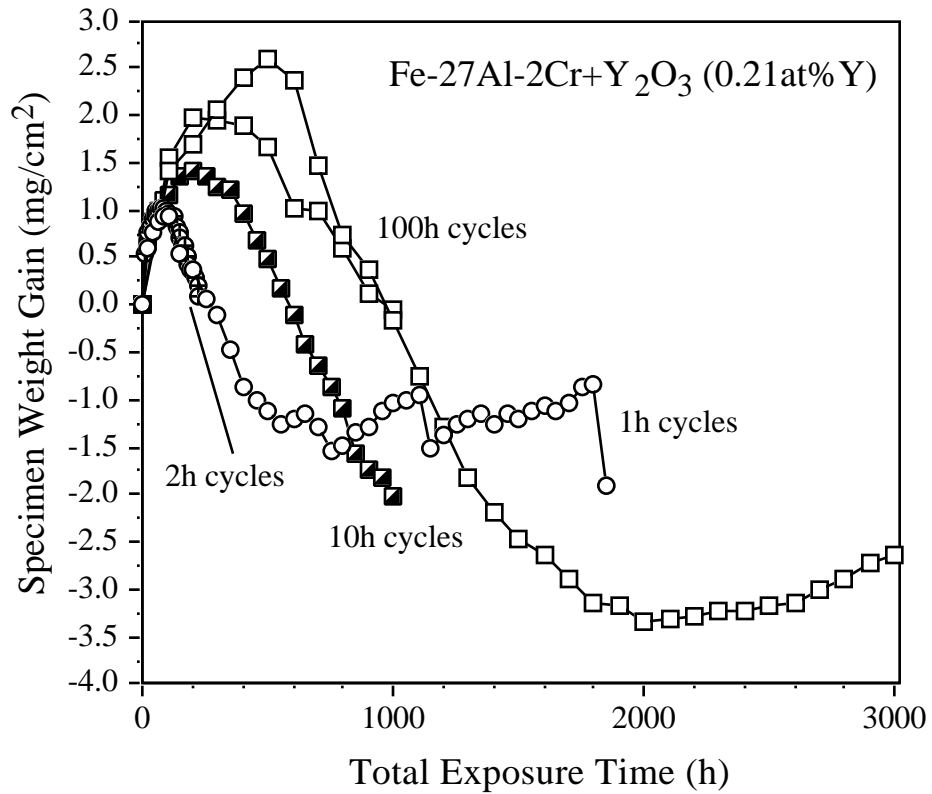


Figure 9. Specimen weight gain for 1.5mm thick ODS Fe₃Al as a function of cycle time at 1200°C. Initially, a lower cycle frequency resulted in less specimen weight loss with time. In 1h cycles, weight loss was arrested when the specimen began to deform and form spinel.

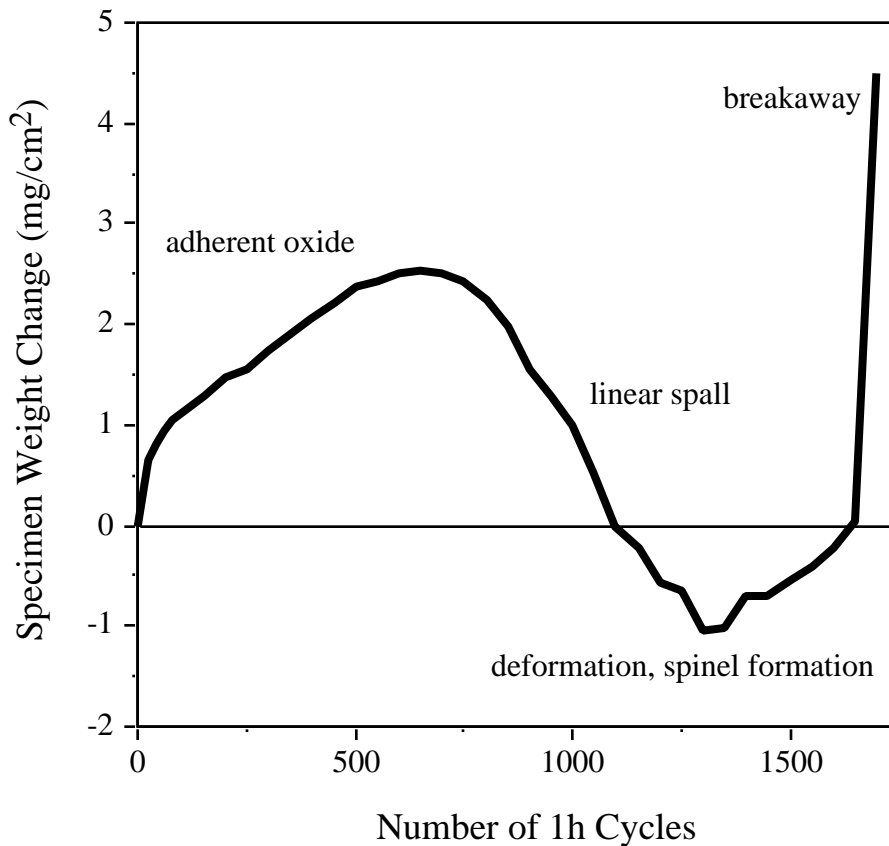


Figure 10. Representative example of specimen weight change for Fe-base alumina-forming alloys in 1h cycles at 1200°C. Behavior tends to follow four periods: (1) adherent oxide formation, i.e. no spallation with weight gains comparable to those measured isothermally; (2) onset of spallation, sometimes following a linear loss, like that observed for Ni-base alloys; (3) substrate deformation (warping or curving) usually accompanied by spinel formation and specimen no longer losing weight and, finally, gaining weight prior to (4) breakaway oxidation, i.e the formation of FeO.

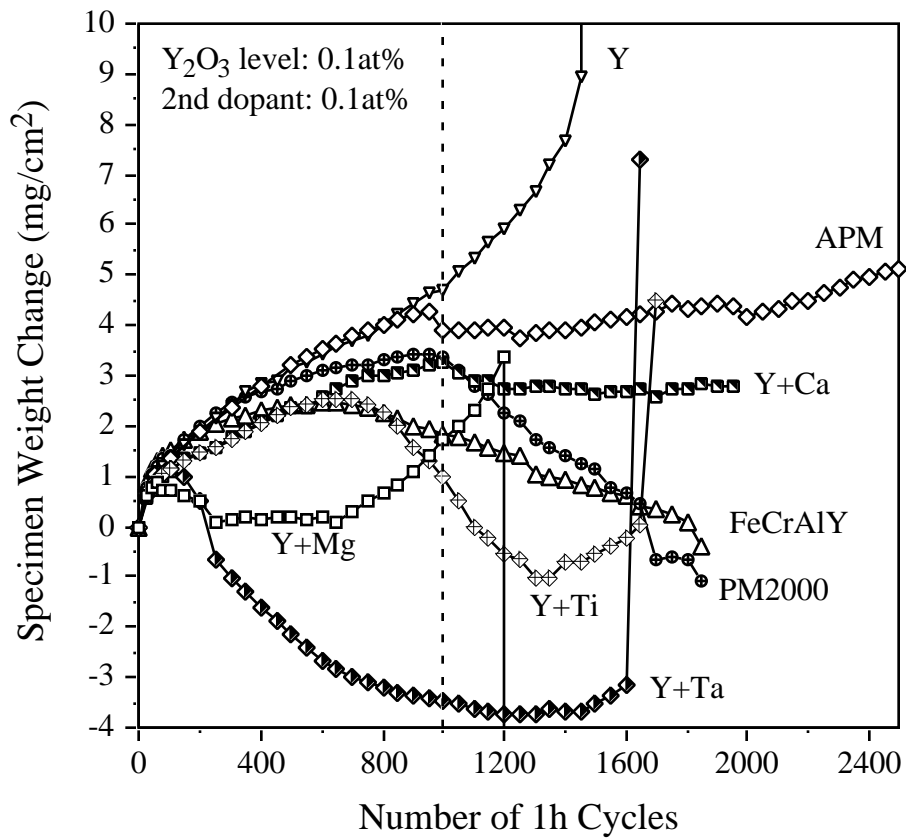


Figure 11. Specimen weight gain for 1.5mm thick FeCrAl alloys in 1h cycles at 1200°C. No simple relationship can explain the range of behaviors observed. Lifetime predictions based on 1000h (dashed line) would fail to predict the behavior of most of these materials. For example, FeCrAl co-doped with 0.1at% Y₂O₃ and 0.1at% Ta₂O₅ initially lost a significant amount of weight but lasted as long as the alloy co-doped with TiO₂. The best alloys require even longer times to begin spallation.

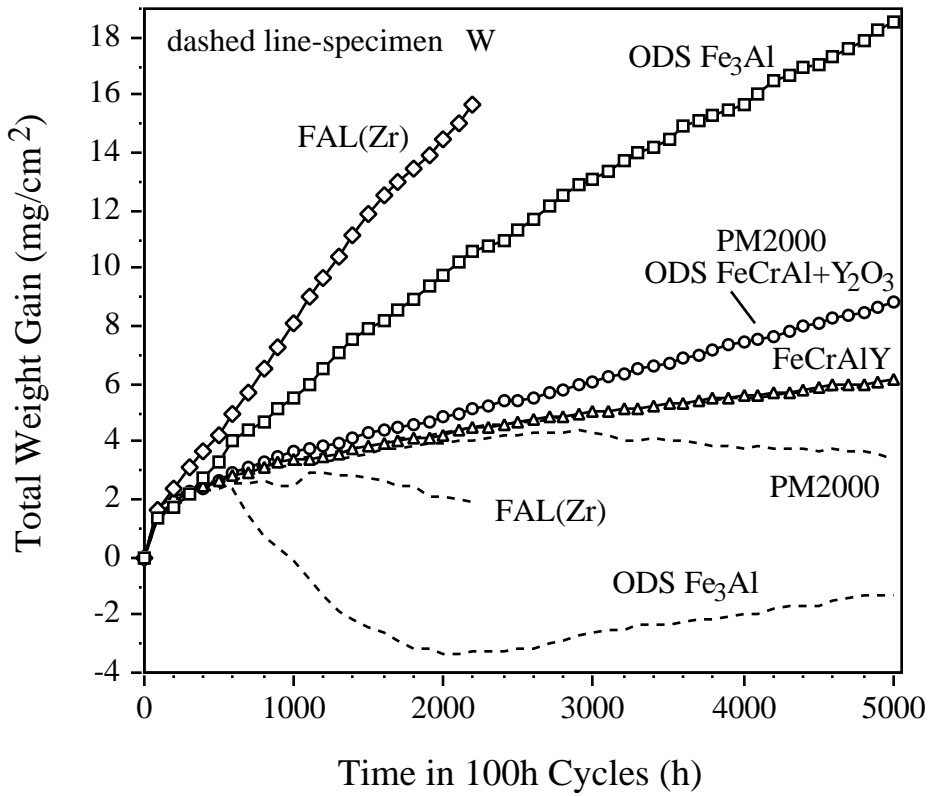


Figure 12. Total and specimen weight gains for several Fe-base alloys in 100h cycles at 1200°C. Whereas there were various behaviors for the specimen weight change, the total weight gains were more well-behaved. The total weight gain is directly proportional to the metal wastage and, therefore, can be used to predict lifetime. No spallation was observed for FeCrAlY as the total and specimen weight gains coincided.

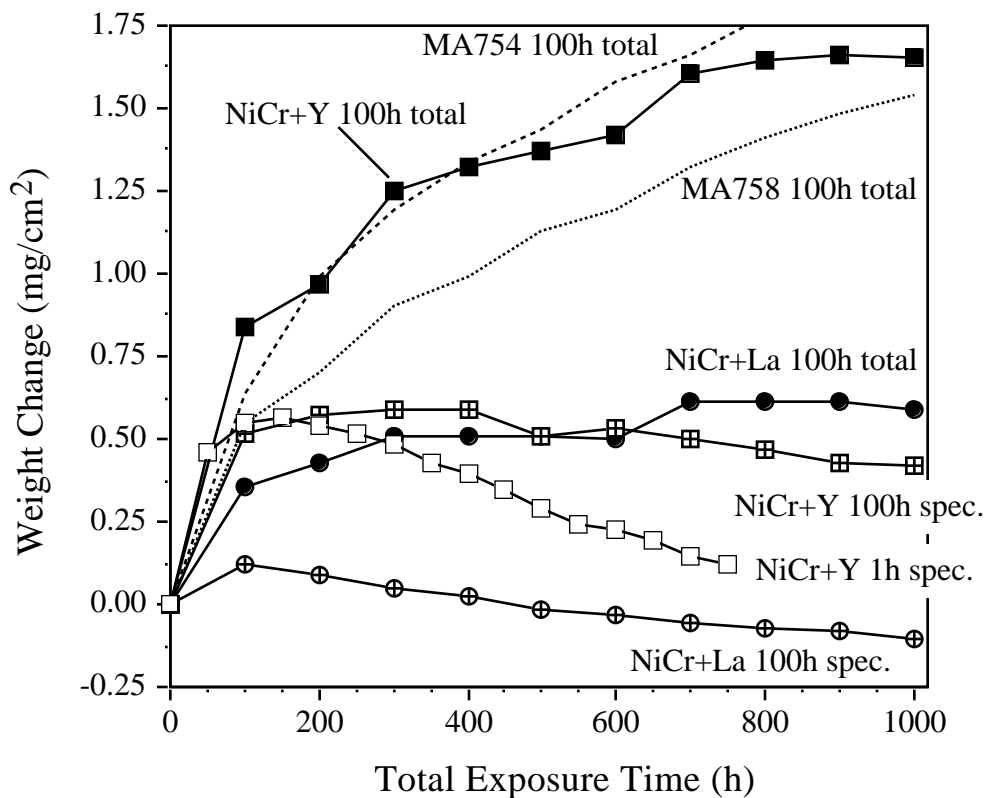


Figure 13. Total and specimen weight gains for several ODS NiCr alloys at 1000°C. In 100h crucible test, specimen weight loss (relative to the total weight gain) for Ni-26Cr+Y₂O₃ and Ni-26Cr+La₂O₃ was attributed solely to CrO₃ evaporation, as no spallation was observed in the crucible. In 1h uncontained cycles, more weight loss was observed, whether this was due to enhanced evaporation outside a crucible or increased spallation is not known. Total weight gains for commercial Y₂O₃-dispersed NiCr alloys MA754 and MA758 are shown to confirm the normal behavior of Y-doped NiCr and the superior performance with La-doping.

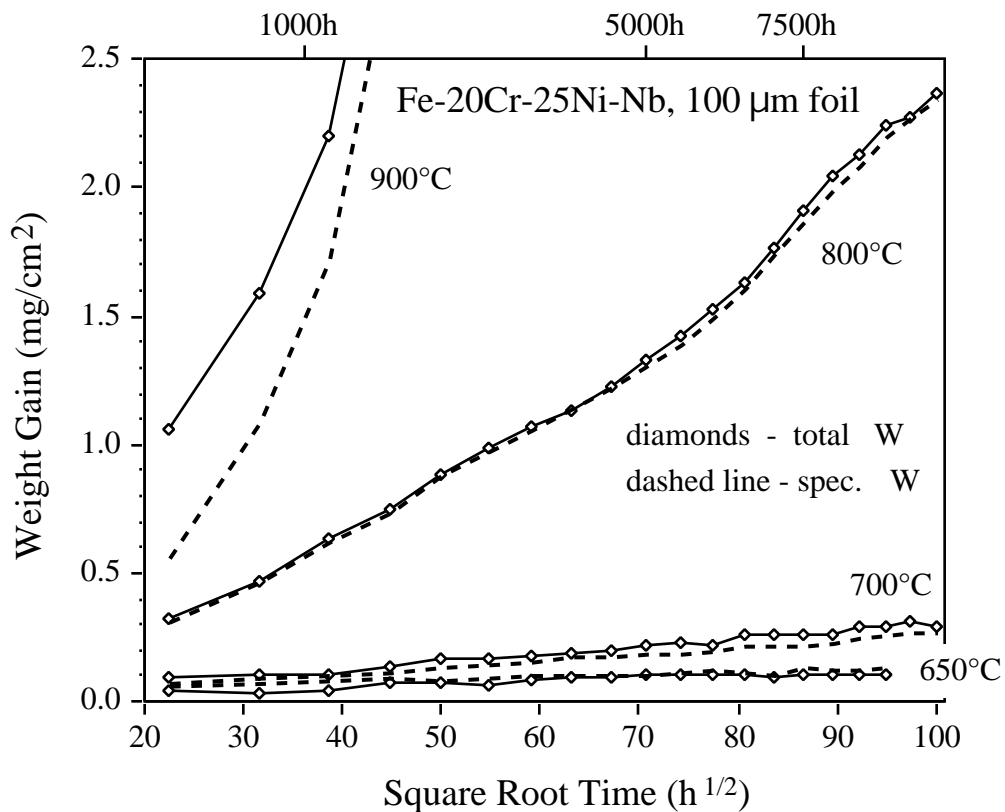


Figure 14. Weight gain for Fe-20Cr-25Ni+Nb 100 μm foil at several temperatures plotted against the square root of time to show the parabolic relationship. The diamonds mark the total weight gain in 500h cycles and the dashed line is the specimen weight gain. Except at 900°C, there was little spallation observed. At 650°C, the total was less than the specimen weight because of an experimental problem.